Single-Channel Properties of I_{Ks} Potassium Channels

Youshan Yang and Fred J. Sigworth

From the Department of Cellular and Molecular Physiology, Yale University School of Medicine, New Haven, Connecticut 06520

ABSTRACT Expressed in *Xenopus* oocytes, KvLQT1 channel subunits yield a small, rapidly activating, voltage-dependent potassium conductance. When coexpressed with the minK gene product, a slowly activating and much larger potassium current results. Using fluctuation analysis and single-channel recordings, we have studied the currents formed by human KvLQT1 subunits alone and in conjunction with human or rat minK subunits. With low external K^+, the single-channel conductances of these three channel types are estimated to be 0.7, 4.5, and 6.5 pS, respectively, based on noise analysis at 20 kHz bandwidth of currents at +50 mV. Power spectra computed over the range 0.1 Hz–20 kHz show a weak frequency dependence, consistent with current interruptions occurring on a broad range of time scales. The broad spectrum causes the apparent single-channel current value to depend on the bandwidth of the recording, and is mirrored in very "flickery" single-channel events of the channels from coexpressed KvLQT1 and human minK subunits. The increase in macroscopic current due to the presence of the minK subunit is accounted for by the increased apparent single-channel conductance it confers on the expressed channels. The rat minK subunit also confers the property that the outward single-channel current is increased by external potassium ions.

KEY WORDS: KvLQT1 • long QT syndrome • fluctuation analysis • minK

INTRODUCTION

Expression of the minK protein is associated with potassium channel activity in a variety of tissues (Busch and Suessbrich, 1997). The minK (also called I_{SK}) protein underlies a slowly activating current in uterine smooth muscle (Boyle et al., 1987) that is developmentally regulated; it also underlies the slow delayed rectifier current I_{Ks} in cardiac tissue (Freeman and Kass, 1993; Varnum et al., 1993) and a potassium current in epithelial cells of the ear (Sakagami et al., 1991; Marcus and Shen, 1994). Expression of this small (129–130 amino acids) protein in heterologous systems yields at most a small potassium current whose magnitude saturates at low expression levels (Lesage et al., 1993; Blumenthal and Kaczmarek, 1994), suggesting that it must combine with other subunit types to form functional I_{Ks} channels. In the channel complex minK appears to be present in multiple copies (Tzounopoulos et al., 1995), quite possibly as few as two (Wang and Goldstein, 1995).

The other partner in the I_{Ks} channel is the product of the LQT1 gene. Long QT syndrome (LQTS)[1] is a genetically heterogeneous disorder that causes cardiac arrhythmias and leads to sudden death. One of several loci for this disorder, LQT1 is located on chromosome 11 (Keating et al., 1991) and is the gene for a potassium channel subunit named KvLQT1 (Wang et al., 1996*b*). Although KvLQT1 subunits produce a potassium current when expressed alone, much larger currents having the slow kinetic characteristics of I_{Ks} are obtained from the coexpression of KvLQT1 and minK subunits (Barhanin et al., 1996; Sanguinetti et al., 1996; Yang et al., 1997). The LQTS-associated mutations in the KvLQT1 gene appear to reduce the expressed I_{Ks} current in a dominant-negative fashion (Shalaby et al., 1997; van den Berg et al., 1997).

Because KvLQT1 subunits give rise to functional potassium channels when expressed alone, it is interesting to consider the nature of the interaction between minK and KvLQT1 that produces larger and more slowly activating currents when these genes are coexpressed. It has been argued that minK serves as a regulator of channel activity (Attali et al., 1993; Ben-Efraim et al., 1996), but evidence is accumulating that minK residues form part of the pore of the I_{Ks} channel complex (Wang et al., 1996*a*; Sesti and Goldstein, 1998; Tai and Goldstein, 1998). In a recent study using COS cells (Romey et al., 1997), it was concluded that the effect of minK coexpression was greatly to increase channel number while decreasing the single-channel conductance of the channels expressed from KvLQT1 subunits. In the present study, we revisit the single-channel properties of the KvLQT1 and coexpressed channels, making use of fluctuation analysis and single-channel recordings from *Xenopus* oocytes. A companion study considers the single-channel properties of coexpressed

Address correspondence to F.J. Sigworth, Department of Cellular and Molecular Physiology, Yale University School of Medicine, 333 Cedar Street, New Haven, CT 06520-8026. Fax: 203-785-4951; E-mail: fred.sigworth@yale.edu

[1]*Abbreviation used in this paper:* LQTS, long QT syndrome.

channels containing mutant minK subunits as well (Sesti and Goldstein, 1998).

MATERIALS AND METHODS

DNA and RNA Synthesis

Human and synthetic rat minK cDNAs (Hausdorff et al., 1991; Goldstein and Miller, 1991) were obtained from Dr. S. Goldstein (Yale University) and propagated in pGEM-A and pBF2 vectors, respectively (Swanson et al., 1990; Tai and Goldstein, 1998). Point mutations in the minK constructs were made by PCR and verified by sequencing. Plasmids of rat and human minK were linearized with NotI and MluI, respectively. cRNAs were transcribed with the MEGAscript T7 and SP6 RNA polymerase kits (Ambion Inc., Austin, TX). Two human KvLQT1 constructs were obtained from Drs. M. Sanguinetti and M. Keating (University of Utah), which we call s-KvLQT1 and l-KvLQT1. The s-KvLQT1 (Sanguinetti et al., 1996) has a truncated NH_2 terminus, while l-KvLQT1 is full-length, having 95 additional residues at the NH_2 terminus (Yang et al., 1997). Each KvLQT1 gene was subcloned into a modified Bluescript vector (Bluescript KSM; gift from W. Joiner, Yale University) that incorporates β-globin untranslated sequences and a poly-A tail for increased protein translation in oocytes. Plasmids of s-KvLQT1 and l-KvLQT1 were linearized with NotI and XbaI, respectively, and transcribed with the MEGAscript T3 RNA polymerase kit (Ambion Inc.). Sizes of transcribed cRNAs were verified by gel electrophoresis.

Electrophysiology

Human KvLQT1 cRNA (5.8 ng) was injected into *Xenopus* oocytes alone or in conjunction with 1 ng minK cRNA. We use the notation hI_{Ks} to denote channels resulting from coexpression of human minK and human KvLQT1, rhI_{Ks} to denote channels from the combination of rat minK and hKvLQT1, and I_{LQT} to denote channels expressed from hKvLQT1 alone. In this study, only the full-length l-KvLQT1 variant was used for expressing hI_{Ks} and I_{LQT} channels; most rhI_{Ks} recordings were made with this variant as well. The rhI_{Ks} channels formed with the truncated s-KvLQT1 construct had identical behavior in terms of voltage dependence and single channel unitary current.

Patch- and voltage-clamp recordings were done at room temperature, 7–12 d after RNA injection. Patch clamp recordings were obtained using EPC-9 (HEKA Electronic, Lambrecht, Germany) or Axopatch 200B (Axon Instruments, Foster City, CA) amplifiers. Pipettes were pulled from 7052 glass (Corning Glass Works, Corning, NY) to a tip size of 2–5 μm. Pipettes with tip diameters of ~30 μm were used for recording I_{LQT} channel currents. These pipettes were pulled from thin-walled borosilicate capillaries (PG165T; Warner Instruments, Hamden, CT). The standard bath solution for patch clamp recordings was (mM) 7 KCl, 93 K-aspartate, 1 EGTA, and 10 HEPES. The standard pipette solution was (mM) 0.2 KCl, 100 NaCl, 1 $MgCl_2$, 1.8 $CaCl_2$, and 10 HEPES. All solutions were titrated to pH 7.4.

For two-microelectrode voltage clamp recordings, an OC-725 amplifier (Warner Instruments) was driven by the Pulse software (HEKA Electronic) and an analogue interface (ITC-16; Instrutech Corp., Mineola, NY). Microelectrodes were filled with 1 M KCl and had 0.1–0.3 MΩ resistance. The standard bath solution for voltage clamp recordings, denoted ND96, contained (mM) 96 NaCl, 2 KCl, 0.1 $CaCl_2$, 1 $MgCl_2$, and 5 HEPES, pH 7.4.

Half-amplitude threshold analysis (Colquhoun and Sigworth, 1995) was used to idealize single-channel recordings for kinetic analysis and the reconstruction of ensemble time courses. For noise analysis, the macroscopic currents induced by a series of depolarizing pulses were recorded on video tape using a VR-10 Digital Data Recorder (Instrutech Corp.). Data were then transferred digitally from tape through the VR-10 Digital Recorder using the program VCatch developed in our laboratory. The raw data (94 kHz sampling rate) were filtered and decimated using a digital Gaussian filter. Power spectra were calculated from data decimated and filtered to 10 Hz, 100 Hz, 1 kHz, and 10 kHz bandwidths. A power spectrum covering the frequency range 0.1 Hz–20 kHz was obtained by combining the four individual spectra after correcting for filter responses.

Statistical quantities are expressed as mean ± SEM with the number of determinations $n \geq 3$ unless otherwise stated.

RESULTS

Activation of I_{Ks} and I_{LQT} Channels

In oocytes coinjected with minK and KvLQT1 cRNAs, both cell-attached and inside-out patch recordings showed slowly activating outward currents with monotonically increasing noise during 5-s depolarizations (Fig. 1, *A* and *B*). As characterized by Boltzmann fits to isochronal conductance–voltage curves, the voltage dependence of activation of these hI_{Ks} and rhI_{Ks} channels is quite shallow, with an effective charge of 1–1.2 e_0 and a midpoint voltage near +55 mV. The main difference in behavior between the two channel types is the more rapid time course of activation in the hI_{Ks} channels. Both channel types show gradually increasing current even at the end of 60-s depolarizations to +50 mV (Fig. 1, *D* and *E*).

For comparison, the activation of currents resulting from the injection of hKvLQT1 cRNA alone is shown from a cell-attached giant patch recording in Fig. 1 *C*. The fragility of the giant patches precluded recordings at large positive voltages, but a Boltzmann fit over the accessible voltage range yields a half-activation voltage of −6 mV, considerably more negative than that of I_{Ks} channels and consistent with previous observations (Sanguinetti et al., 1996). The tail currents show a "hook" in the time course, characteristic of KvLQT1 currents (Sanguinetti et al., 1996; Pusch et al., 1998). The patch recordings shown in Fig. 1 all have similar kinetics and voltage dependence to the corresponding whole cell-currents obtained by two-electrode voltage clamp.

Reversal potentials of rhI_{Ks} currents were measured from macroscopic tail currents obtained in inside-out or cell-attached patch recordings with 100 mM K^+, Na^+, Rb^+, or Cs^+ in the pipette; in each case, the bath solution contained 100 mM K^+. Table I (*top*) shows the reversal potentials of the rhI_{Ks} channels. The table also gives the computed permeability ratios. The permeability ratios are very similar to those obtained from voltage clamp recordings of oocytes injected with rat minK RNA (Hausdorff et al., 1991). Like many other potassium channels, the permeability sequence is $K^+ > Rb^+ > Cs^+ > Na^+$.

It was more difficult to obtain patch recordings with macroscopic hI_{Ks} currents. Therefore, the ion selectiv-

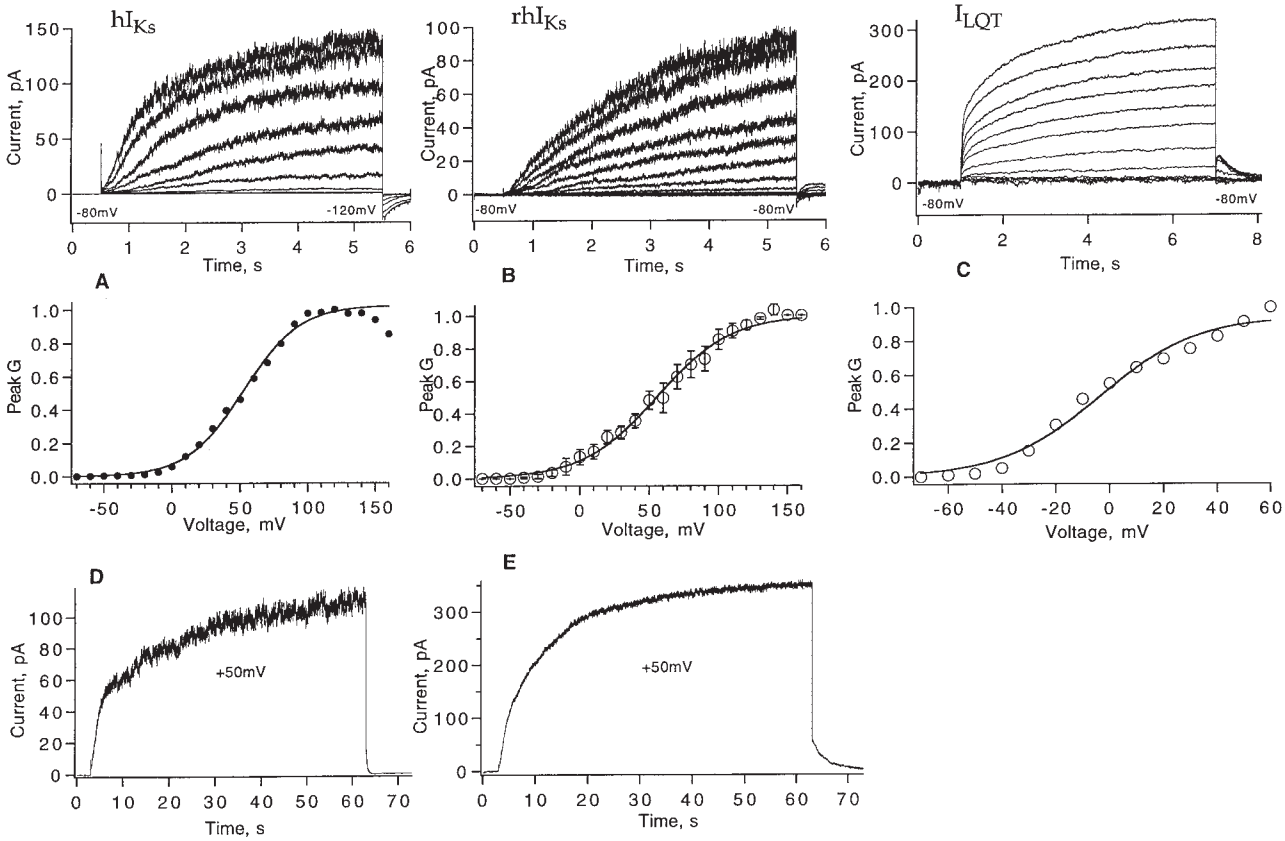

FIGURE 1. Macroscopic currents from the channel types hI_{Ks} (from human minK coexpressed with hKvLQT1), rhI_{Ks} (rat minK coexpressed with hKvLQT1), and I_{LQT} (hKvLQT1 expressed alone). (*A*) Activation of human I_{Ks} currents from a cell-attached patch recording with standard patch solutions. Currents (*top*) were induced by depolarizations to −70 to +110 mV in 20-mV steps from a −80-mV holding potential. No leak subtraction, filtered at 500 Hz. The isochronal voltage dependence of normalized conductance (*bottom*) was fitted with a Boltzmann function $G = G_{max}/(1 + \exp[(V_{1/2} - V)/k]$, with $V_{1/2} = 52$ mV and $k = 20$ mV. (*B*) Activation of rhI_{Ks} currents from an inside-out patch recording with 130 mM K-aspartate, 10 mM KCl, 1 mM EGTA, pH 7.4 in the bath; 100 mM NaCl, 0.2 mM KCl, 1 mM $MgCl_2$, 1.8 mM $CaCl_2$, pH 7.4 in the pipette. Current activation (*top*) at −70 to +150 mV in 20-mV steps from −80-mV holding potential. Leak current was subtracted by the P/5 protocol with −100-mV leak holding potential; data were filtered at 500 Hz. The isochronal voltage dependence of rhI_{Ks} from three patches is fitted by a Boltzmann function with $V_{1/2} = 56$ mV and $k = 26$ mV. (*C*) Activation of I_{LQT} from a giant patch (30-μm diameter pipette tip) with 93 mM K-aspartate, 7 mM KCl, 1 mM EGTA, pH 7.4 in the bath, 96 mM NaCl, 2 mM KCl, 1 mM $MgCl_2$, 0.1 mM $CaCl_2$, pH 7.4 in the pipette. Currents were induced by depolarizing pulses from a −80-mV holding potential to potentials of −70 to +60 mV in 10-mV steps, and repolarization to −60 mV; filtered at 100 Hz. No leak current correction was applied. Normalized peak conductance was fitted with $V_{1/2} = -6$ mV and $k = 18$ mV. Conductance in all three cases was computed assuming a linear open-channel current–voltage relationship with a reversal potential of −80 mV. (*D*) hI_{Ks} current from a cell-attached patch recording with standard solutions, showing the response to a 60-s depolarization to +50 mV. Filter bandwidth 40 Hz. (*E*) A corresponding recording of rhI_{Ks} current.

ity of these channels was characterized from whole cell currents with 100 mM K^+, Na^+, Rb^+, or Cs^+ in the bath solution. For comparison, the reversal potentials of rhI_{Ks} channels were also measured in this way, using the same batch of oocytes. There was no significant difference in reversal potentials between these two channel types (Table I).

Single hI_{Ks} Channel Current

If we assume that the I_{Ks} channel only has one conductance level with unitary current i, then for n channels the variance of current fluctuations will depend on the mean current I according to

$$\sigma^2 = Ii - \frac{I^2}{n} \quad (1)$$

(Sigworth, 1980). We shall denote by i_v an estimate of i obtained from fitting Eq. 1 to the variance–mean relationship. For this analysis, a series of current sweeps was collected by applying repetitive depolarizing pulses to +50 mV. The mean current and variance from hI_{Ks} channels (Fig. 2 *A*) were computed using groups of two sweeps to minimize errors due to slow current drifts (Heinemann and Conti, 1992). Shown in Fig. 2, *B* and *C*, are two mean–variance plots computed from data filtered to different extents. Fitting Eq. 1 yielded the estimates $i_v = 0.28$ pA at 100 Hz and 0.51 pA at 10 kHz

TABLE I

Reversal Potential V_r of I_{Ks} Channels with Various External Ions

Conditions	K^+	Rb^+	Cs^+	Na^+
rhI_{Ks} patch clamp ($n = 3$)	-1.5 ± 0.5	-7.3 ± 0.6	-73 ± 0.7	<-110
rhI_{Ks} voltage clamp ($n = 6$)	-1.2 ± 0.6	-11 ± 0.4	-61 ± 0.3	-110 ± 1.2
hI_{Ks} voltage clamp ($n = 9$)	-1.2 ± 0.2	-10 ± 0.2	-60 ± 0.4	-108 ± 0.7
rhI_{Ks} P_X/P_K (patch, $n = 3$)	1	0.75 ± 0.03	0.06 ± 0.003	$<0.01 \pm 0.002$

Reversal potentials (in millivolts) were estimated from inside-out or cell-attached patch clamp recordings or from two-electrode voltage clamp. The pipette solution contained 100 mM of test cation X; bath solution contained 100 mM K^+. For voltage clamp measurements, reversal potentials were obtained using 100 mM of the test cation in the bath solution. The relative permeability of rhI_{Ks} to ion X (*bottom row*) was calculated as $P_X/P_K = \exp(F\Delta V_r/RT)$, where $\Delta V_r = V_r(X) - V_r(K)$, as obtained from patch recordings.

bandwidth. The discrepancy between the two estimates of unitary current suggests that a substantial amount of variance is contained in high-frequency components.

To investigate the high-frequency components of the hI_{Ks} current fluctuations, we computed the power spectrum of the macroscopic currents. Pairs of aligned current traces were subtracted as shown in Fig. 2 *D*. Power spectra were computed from subtracted traces (Sigworth, 1981) by fast Fourier transform and the resulting power spectrum after correction for background noise is shown in Fig. 2 *E*. It has a remarkably straight $1/f$ dependence over five decades of frequency. The weak frequency dependence of the spectral density implies that the observed noise variance will be heavily dependent on filter cutoff frequency. From Parseval's theorem, we have

$$\sigma^2 = \int_0^\infty S(f)\,|H(f)|^2 df, \qquad (2)$$

where $S(f)$ is the power spectral density of the current fluctuations and $H(f)$ is the filter transfer function. To give an idea of the effect of filter bandwidth, the spectral density in Fig. 2 *E* was integrated numerically and converted into unitary current amplitude according to the expression

$$i_s(f) = \bar{I}^{-1} \int_0^f S(f')\,df', \qquad (3)$$

where $\bar{I}$ is the time-averaged mean current and $i_s(f)$ is the apparent unitary current at bandwidth f. As can be seen in Fig. 2 *F*, i_s increases strongly with filter bandwidth, and is still increasing at $f = 20$ kHz. Thus, fluctuation analysis is expected to yield any of a variety of unitary current amplitudes, depending on the bandwidth. At 20 kHz, i_s is 0.47 pA at +50 mV.

The expression in Eq. 3 is missing a correction term (Sigworth, 1981) and therefore underestimates the unitary current by a factor of about $1 - \bar{p}$, where $\bar{p}$ is the mean open probability. Thus, the apparent unitary currents from spectral analysis (Fig. 2 *F*) of 0.2 and 0.47 pA, at 100 Hz and 20 kHz bandwidth, respectively, become ~0.25 and 0.6 pA when $\bar{p} = 0.2$ is assumed. These values agree with those obtained from the mean–variance analysis (Fig. 2, *B* and *C*).

Unitary currents roughly 0.5 pA in size should be visible in single-channel recordings. Obtaining single-channel patches was difficult, however, because the hI_{Ks} channels appeared to be highly clustered in the oocyte membrane so that patches typically contained either tens of channels or no channels at all. The distribution of patch current density was very broad, as determined from more than 100 patches (Fig. 3). Fig. 4 *A* shows one of our best candidates for an hI_{Ks} single-channel current. This sweep was recorded from a multiple-channel patch but appears to have only one channel active. As would be expected from the very broad power spectrum of macroscopic current fluctuations, the channel current shows very rapid flickering. From recordings at three voltages, the single-channel conductance is estimated to be 3 pS at 200 Hz bandwidth (Fig. 4 *C*).

Conductance of I_{LQT} Channels

Injection of the KvLQT1 cRNA alone results in small K^+ currents having more rapid kinetics than I_{Ks} channels. Might the smaller current result from smaller single-channel currents? In the case of the hI_{Ks} channels, mean–variance and spectral fluctuation analysis yielded reasonable estimates of the unitary current at +50 mV, comparable to what was observed in a patch recording. To determine the I_{LQT} unitary current, we used the same fluctuation-analysis methods and similar experimental protocols. The only difference was that in attempting to record those currents, we encountered a very low channel density. Using pipettes with 2–5-μm tip diameters, we saw no current in 12 patches from oocytes having mean whole-cell currents of 4 μA. Therefore, we used much larger pipettes (30-μm tip diameter) to obtain macroscopic channel currents. Fig. 5 *A* shows one cell-attached giant patch having a mean current of 240 pA at +50 mV. This recording shows the characteristic "hook" of outward tail current that is seen in I_{LQT} channels. The mean–variance relationship, computed from data filtered at 200 Hz, is poorly fitted

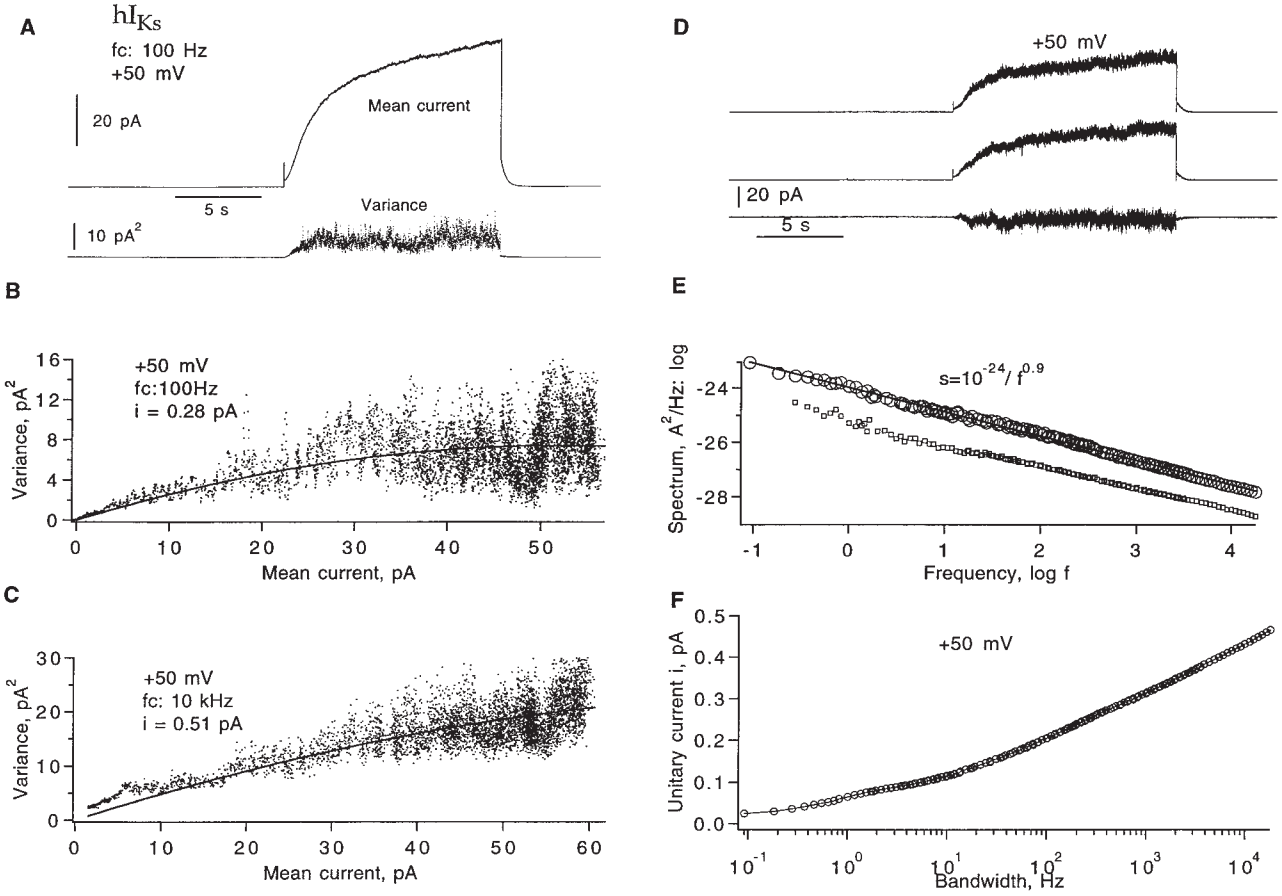

FIGURE 2. Fluctuation analysis of hI_{Ks} currents. (*A*) Mean current and time-dependent variance computed from 30 sweeps filtered at 100 Hz. The current was induced by +50-mV depolarizing pulses from a −80 mV holding potential in a cell-attached patch recording. Pulses were delivered every 32 s. (*B*) Mean–variance plot of 100 Hz–filtered currents. A fit of Eq. 1 yields unitary current $i_v = 0.28$ pA and number of channels (n) = 368; the corresponding apparent open probability $P_{max} = 0.43$. (*C*) Mean–variance plot from a total of 20 sweeps at 10 kHz bandwidth from the same patch. In this case, 12-s depolarizations to +50 mV were delivered every 32 s. The fit yields $i_v = 0.51$ and $P_{max} = 0.24$. (*D*) A pair of successive current traces and their difference filtered at 1 kHz; same set of data as in *A*. (*E*) The top trace is the resulting power spectrum of currents from 30 sweeps after correction for background noise. The contribution S_{shot} from ion transport during channels opening was estimated according to $S_{shot} = 2e_0I = 1.4 \cdot 10^{-29}$ A²/Hz and was subtracted. The solid line indicates a power-law fit $S(f) = 10^{-24}/f^{0.9}$ A²/Hz. The mean current was 45 pA, and the unitary current estimate $i_s = 0.47$ pA at 20 kHz bandwidth. The lower trace shows the spectrum (values plotted one decade lower in the graph for clarity) computed from another representative data set, where the mean current was 39 pA; the unitary current $i_s = 0.44$ pA at 20 kHz. (*F*) Dependence of apparent unitary current i_s (Eq. 3) on filter cut-off frequency at +50 mV. Variance was calculated from the numeric integral of the power spectrum over the frequency range 0.1 Hz–10 kHz.

by the parabolic function of Eq. 1; however, linear fits are consistent with unitary currents of 0.03–0.04 pA, as is shown in Fig. 5 *C*.

Spectral analysis of the fluctuations was also performed. The spectrum shows several discernible components, and can be well fitted by the sum of three Lorentzian functions (Fig. 5 *E*). The integral of the spectrum, scaled to show the apparent unitary current, shows i_s increasing with bandwidth but possibly reaching a limiting value of ~0.09 pA at 20 kHz. The unitary current is therefore about one fifth of that of the hI_{Ks} channels. We were not able to obtain any convincing single-channel recordings of this current.

Single Channel Properties of rhI_{Ks} Channels

We also studied channels formed by coexpression of rat minK with human KvLQT1 subunits. The currents from these channels (Fig. 1) show similar noise properties and voltage dependence to those containing human minK subunits. Fig. 6 shows the fluctuation analysis of these channels. The power spectrum (Fig. 6 *B*) does not have the simple power-law frequency dependence of the hI_{Ks} channels, but can be fitted by one $1/f$ component plus several Lorentzian components, where a minimum of four Lorentzians was required for a good fit. The presence of discernible Lorentzians suggests that rhI_{Ks} channels may have more clearly distin-

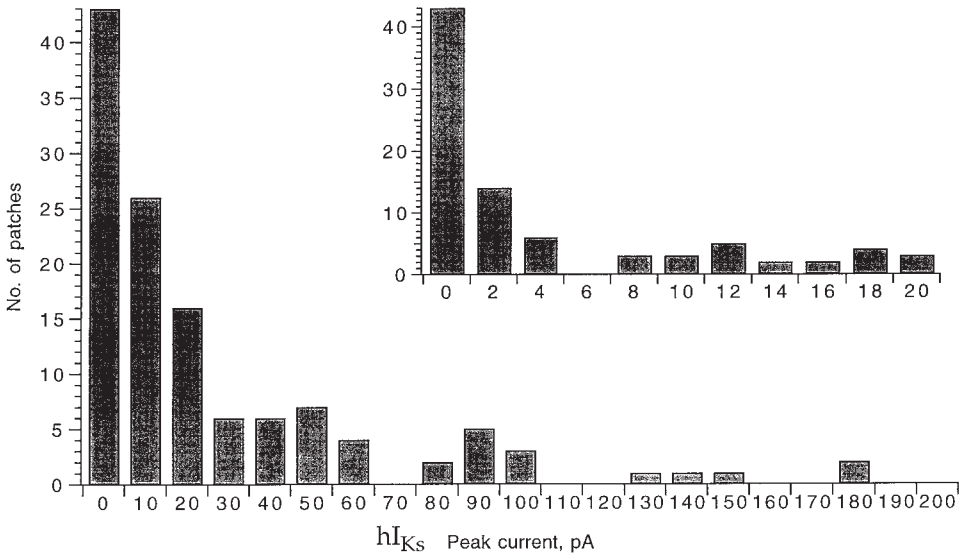

FIGURE 3. Frequency distribution of hI_{Ks} patch currents. Current was measured at the end of a 5-s depolarization to +50 mV in each of 128 patches, and histograms were constructed. The inset shows an expanded histogram, where the bin at zero represents the 43 patches that showed no I_{Ks} current.

guishable kinetic states than hI_{Ks} channels. The unitary current i_s was calculated from the power spectrum from this experiment. Again, i_s shows a strong dependence on bandwidth, as shown in Fig. 6 *C*, with an estimated unitary current of 0.67 pA at 20 kHz. Depending on the estimated open probability, this value should be increased somewhat, for example to 0.84 pA assuming $\bar{p} = 0.2$.

The mean–variance analysis was also applied to same set of data. The fit of Eq. 1 to the mean–variance plot (Fig. 6 *E*) yields an estimate of the unitary current i_v of ~0.28 pA at 100 Hz bandwidth. This is similar to the value obtained from hI_{Ks} channels at this bandwidth.

The presence of discernible Lorentzian components in the power spectrum suggests that the rhI_{Ks} channels should show less flickering than the hI_{Ks} channels. Patch recordings indeed showed single-channel events, but as was the case with hI_{Ks} channels, of >200 trials, we were unable to obtain a one-channel recording of sufficient duration to allow kinetic analysis. Shown in Fig. 7 is a recording from a patch containing three channels using pulses to +50 mV. Channels open after a latency of a few seconds, often first to a subconductance level before reaching the full single-channel current (Fig. 7 *B*). To verify that these channel events correspond to the macroscopic currents, we computed the channel open probability from the idealizations of 60 sweeps. It has a slowly activating time course that reaches an open probability of 0.45 at the end of the 5-s depolarization. This time course superimposes well on the time course of current in a multichannel patch (Fig. 7 *C*). The time

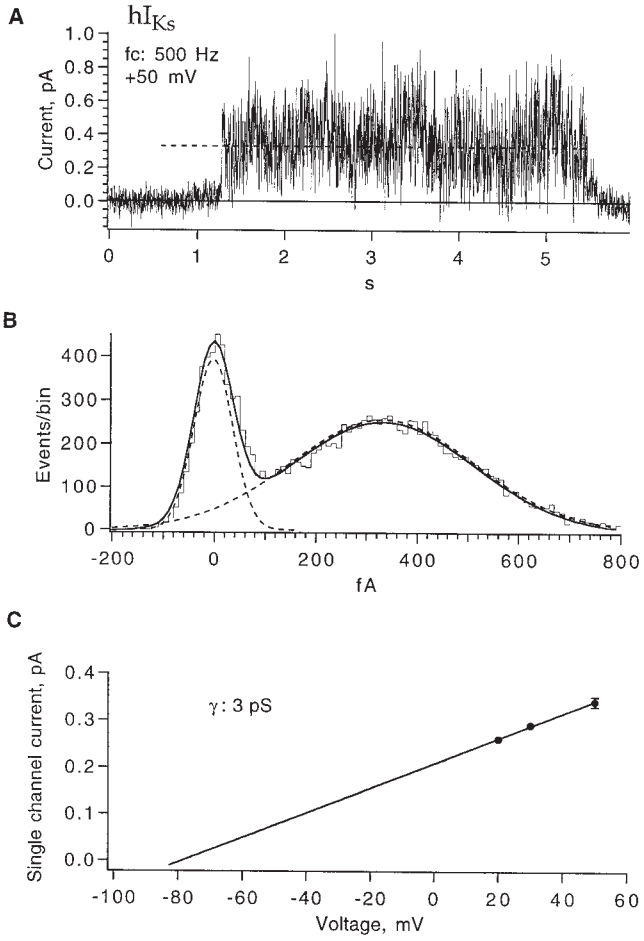

FIGURE 4. Single-channel hI_{Ks} current. (*A*) One sweep showing a putative hI_{Ks} single-channel opening, recorded from a three-channel patch at +50 mV. Data were filtered at 500 Hz. (*B*) All-points amplitude histogram, which yields an apparent unitary current 0.34 pA (indicated by the dashed line in *A*). (*C*) Single channel currents estimated from amplitude histograms at 200 Hz bandwidth ($n = 4$ for +50 mV, $n = 1$ for other voltages). A linear fit yields 3 pS for the single-channel conductance.

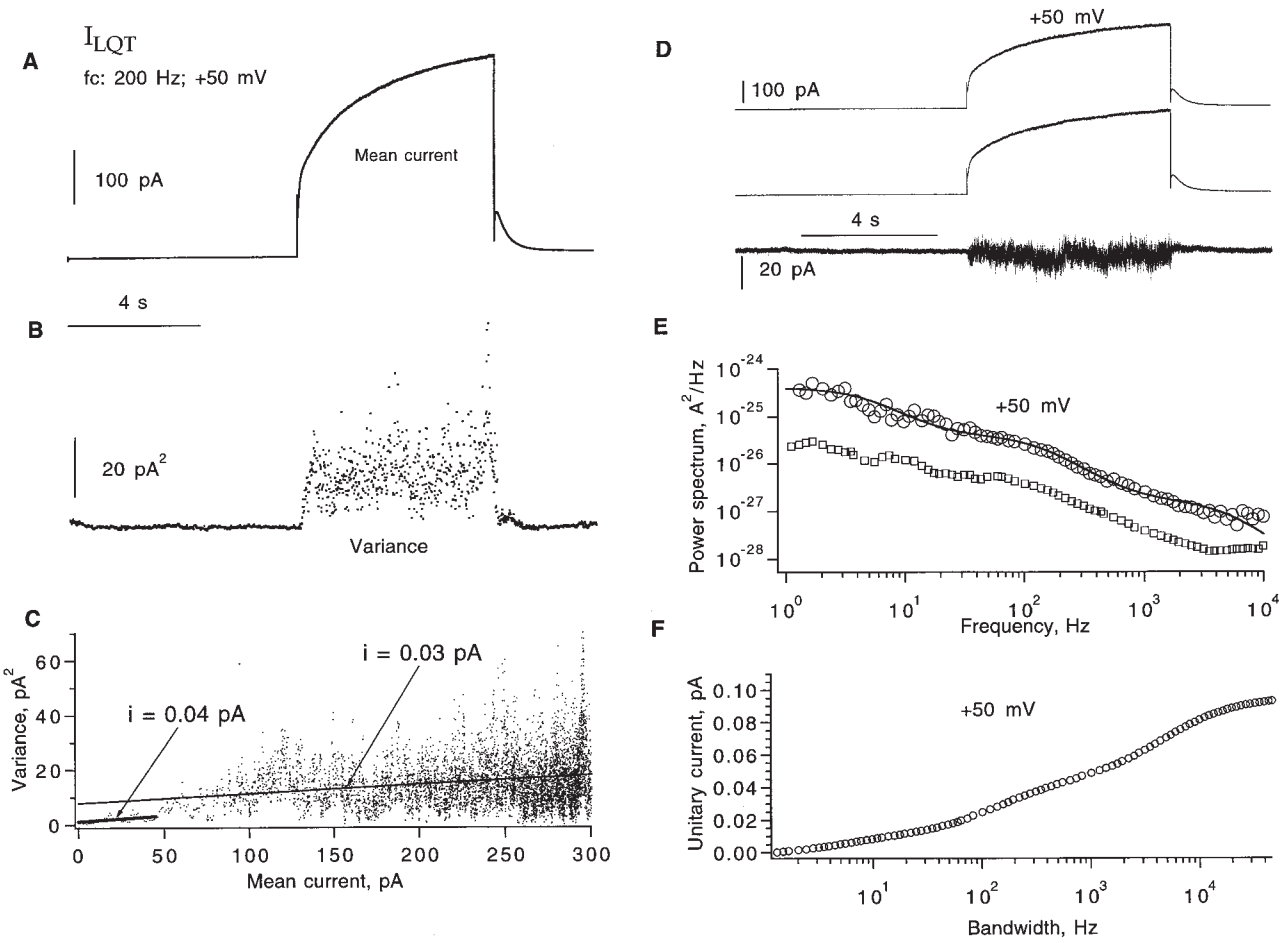

FIGURE 5. Fluctuation analysis of I_{LQT}. (*A*) Ensemble mean current was calculated from pairs of sweeps from a total of 10 sweeps, obtained in a giant cell-attached patch recording from an oocyte injected with KvLQT1 RNA alone. Currents were induced by depolarizing pulses to +50 mV from a −80-mV holding potential and repolarized to −60 mV. Data were filtered at 200 Hz. (*B*) Time course of variance. (*C*) Variance–mean plot. A linear fit for the current range <50 pA yields unitary current i_v = 0.04 pA; i_v = 0.03 pA from a linear fit to the entire current range. (*D*) A pair of aligned current traces and the subtracted current trace filtered at 1 kHz. Same data as in *A*. (*E*) Power spectrum calculated from subtracted currents after background noise subtraction. Solid curve is the sum of three Lorentzians with corner frequencies 5, 141, and 5,000 Hz and amplitudes $3.6 \cdot 10^{-25}$, $3.7 \cdot 10^{-26}$ and $1.6 \cdot 10^{-27}$ A^2/Hz, respectively. The corresponding mean current was 240 pA, and the estimated single-channel current i_s = 0.09 pA at 20 kHz. The bottom trace is the spectrum from another recording, displaced downward by one decade for clarity. The mean current in this case was 370 pA and i_s(20 kHz) = 0.08 pA. (*F*) Unitary current i_s was calculated from the integral of the power spectrum; points beyond 10 kHz were computed from the fitted function. In the patch recording, the bath solution was 93 mM K-aspartate, 7 mM KCl, 1 mM EGTA, 10 HEPES, pH 7.4; the pipette solution contained 100 mM NaCl, 1 mM $MgCl_2$, 0.1 mM $CaCl_2$, 5 mM HEPES.

course of activation can be described by the distribution of first latencies to channel opening. Ignoring the subconductance levels, we measured the first latency to the fully open state and corrected it for the presence of three channels (Aldrich et al., 1983). When scaled by the factor 0.8, it matches very well the time course of the open probability. This correspondence is consistent with the idea that, once a channel opens, it remains open with a substantial probability (apparently 0.8 at this time resolution).

Slow variations in single-channel activity were observed in this patch, with occasional null sweeps (Fig. 7 *B, middle*) occurring throughout the recording (Fig. 7 *F*). A subsequent recording at +20 mV from the same patch (Fig. 8) shows similar kinetic behavior of the single channels. Again, subconductance levels are sometimes seen to precede the full opening of the channel (Fig. 8 *A*) and the slow time course of activation is explained by long first latencies (Fig. 8 *B*). At this smaller depolarization, a higher frequency of null sweeps was seen (Fig. 8 *C*).

External Potassium Dependence of I_{Ks} Channels

The conductance and gating of some types of K^+ channels depend on external K^+ concentration. We tested

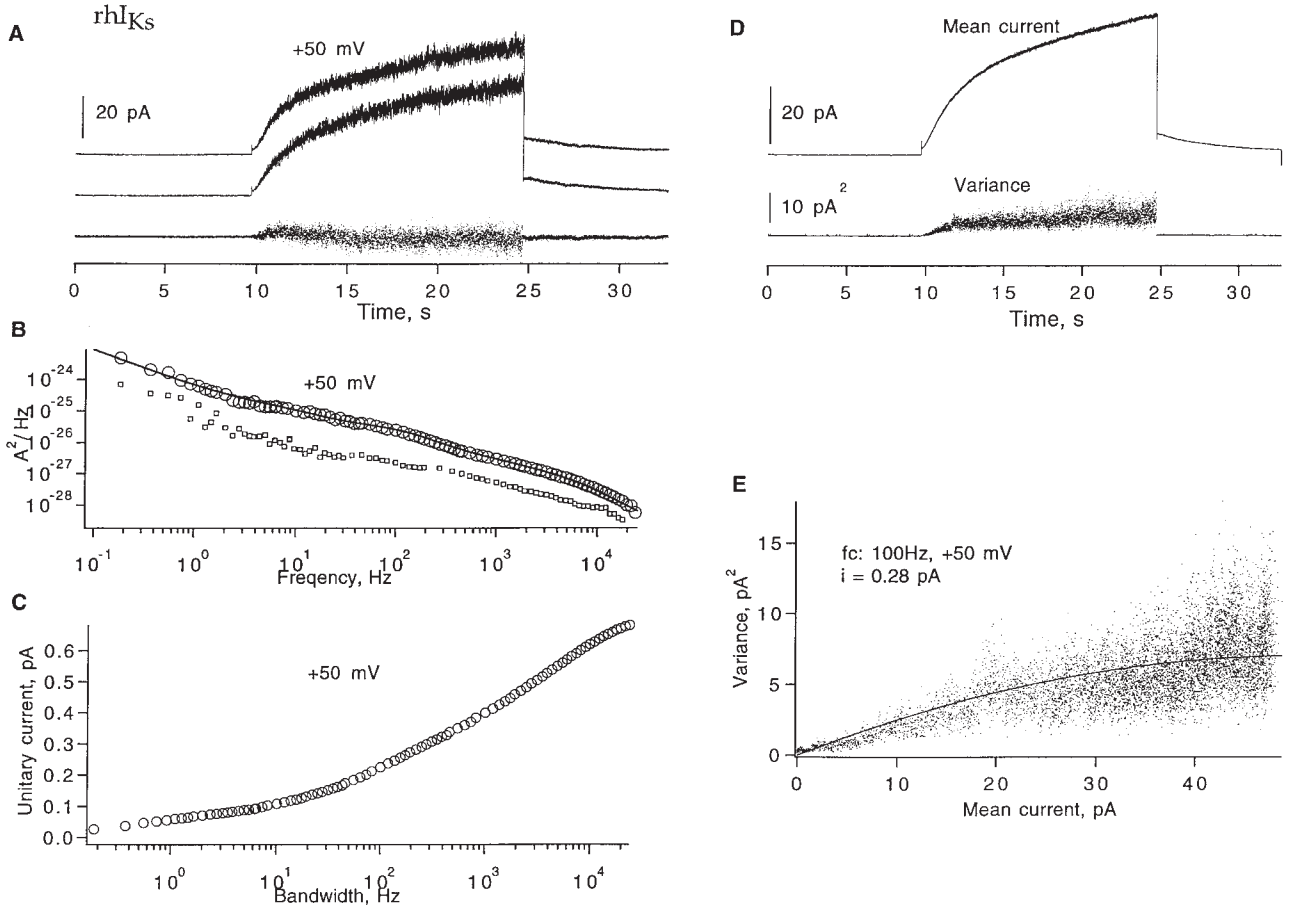

FIGURE 6. Fluctuation analysis of rhI$_{Ks}$ currents. (*A*) A pair of successive current traces, filtered at 1 kHz. The current was induced by +50-mV depolarizing pulses from −80-mV holding potential, and repolarized to –60 mV in a cell-attached patch recording with 140 mM K-aspartate, 1 mM EGTA, 10 mM HEPES, pH 7.4 in the bath; 96 mM NaCl, 2 mM KCl, 1 mM $MgCl_2$, 0.1 mM $CaCl_2$, 5 mM HEPES in the pipette. Pulses were delivered every 33 s; mean current during the depolarizing pulse was 34 pA. (*B*) The corrected power spectrum of currents, computed from 36 traces. The solid curve is a fitted power-law function plus four Lorentzian components, of the form $S = 1.1 \cdot 10^{-29} + 6.1 \cdot 10^{-25}/f^{1.2} + 6 \cdot 10^{-26}/[1 + (f/11)^2] + 2.9 \cdot 10^{-27}/[1 + (f/141)^2] + 2.2 \cdot 10^{-27}/[1 + (f/1{,}195)^2] + 8.8 \cdot 10^{-28}/[1 + (f/3{,}535)^2]$, where f is in Hz and S is in A^2/Hz. The unitary current $i_s = 0.67$ pA at 20 kHz bandwidth. The lower trace is the spectrum from another recording in which the mean current was 7 pA and $i_s = 0.51$ pA at 20 kHz. (*C*) Frequency dependence of unitary current calculated from the numeric integral of power spectrum over the frequency range 0.1 Hz–20 kHz. (*D*) Ensemble mean current and variance, from the same data filtered at 100 Hz. The variance trace was calculated from pairs of sweeps to minimize error due to drift. (*E*) Mean–variance plot. Superimposed is a parabolic fit, which yields the unitary current estimate $i_v = 0.28$ pA.

the external potassium dependence of whole-cell currents using continuous bath perfusion. Fig. 9 shows currents at +30 mV as the bath solution was switched between 0.2 and 10 mM K^+. The hI$_{Ks}$ and rhI$_{Ks}$ channels have opposite responses to the change in external potassium. Switching from 0.2 to 10 mM K^+ reduces the hI$_{Ks}$ current by 20%, an effect that can be explained by the decrease in driving force; however, there is a 20% current increase under the same conditions with rhI$_{Ks}$ channels. That higher external potassium increases outward current was also observed in the I$_{Kr}$ current through HERG channels (Sanguinetti et al., 1995). The effect of external K^+ was also tested for I$_{LQT}$ channels (Fig. 9 *C*). In this case, the currents were smaller when external K^+ was increased. These experiments show that coexpression with the rat minK gene product changes the sensitivity the I$_{LQT}$ channels to external potassium.

A comparison of the human and rat minK sequences (Murai et al., 1989; Fig. 9 *D*) shows many differences in the extracellular (NH_2-terminal) and intracellular (COOH-terminal) regions, but only one nonconserved residue in the putative transmembrane domain. As a first attempt to locate the region responsible for the differences in K^+ sensitivity, we made complementary mutations at this position. The resulting constructs, human (V47I) and rat (I48V) minK were coexpressed with human KvLQT1 and the external potassium sensitivity was

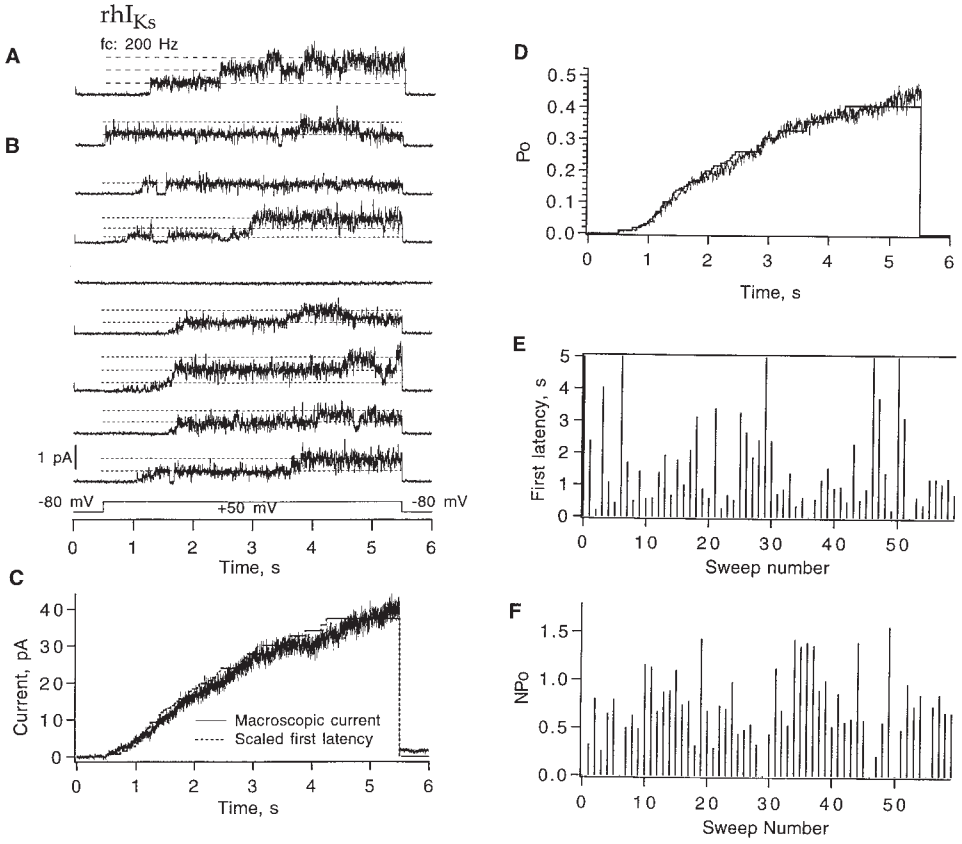

FIGURE 7. A three-channel, inside-out patch recording from rhI$_{Ks}$ channels. (*A*) A trace with three channels opening during +50-mV depolarization. (*B*) Eight successive sweeps from the same patch, showing long first latencies in response to depolarizations to +50 mV from the −80-mV holding potential. Pulses were delivered every 8 s. Data were filtered at 200 Hz. (*C*) Comparison of the time course of the rhI$_{Ks}$ macroscopic current seen in another patch (*noisy trace*) and the first latency function at +50 mV. (*D*) The ensemble mean time courses of open probability at 50 mV obtained from 60 sweeps. The open probability at the end of the 5-s depolarization was ~0.5. The superimposed step-wise curve is the first-latency distribution F_1 scaled by the factor 0.8. It was computed according to $F_1 = 1 - \sqrt[3]{1 - F_3}$, where F_3 is the observed first-latency distribution from 60 sweeps recorded from the three-channel patch. (*E*) Diary plot of the three-channel first latency F_3 in the patch recording. Latency values of 5 s correspond to the case in which no channel opens. (*F*) Diary plot of the time-averaged open probability from this patch. For this recording, the bath solution was 130 mM K-aspartate, 10 mM KCl, 1 mM EGTA, 10 mM HEPES, pH 7.4; the pipette solution was 100 mM NaCl, 0.2 mM KCl, 1 mM $MgCl_2$, 1.8 mM $CaCl_2$, 5 mM HEPES, pH 7.4.

assayed by the ratio of peak current in 10 mM external K^+ to that in 0.2 mM K^+ (Table II). The mutation in human minK had no significant effect on the K^+ sensitivity, but, with the rat mutation increased, K^+ significantly decreased the current ($P < 0.01$), which is the opposite effect to that seen with the wild-type rat minK subunit. Thus, this residue in the membrane-spanning region appears to contribute to the external potassium sensitivity.

Because the single-channel rhI$_{Ks}$ currents can be resolved in patch-clamp recordings, it should be possible to examine the origin of the increase in outward current in these channels when extracellular potassium concentration is increased. Fig. 10 *A* shows three representative single-channel currents from inside-out patches at +50 mV and filtered at 100 Hz. The currents were estimated to be 0.56, 0.44, and 0.37 pA with $[K]_o$ equal to 10, 0.2, and 0 mM. The single-channel current is seen to increase when $[K]_o$ increases, even as the driving force decreases. Recordings from six patches show increased conductance over the voltage range of −30 to +80 mV with higher $[K]_o$ (Fig. 10 *B*). The $[K]_o$ dependence of conductance appears to saturate above 2 mM, and its magnitude accounts for all of the increase in macroscopic current observed on raising extracellular potassium in the case of the rhI$_{Ks}$ channel.

DISCUSSION

This study has considered the single-channel properties of I$_{Ks}$ channels obtained from the coexpression of the human or rat minK protein with human KvLQT1, and has compared these properties with the expression of KvLQT1 subunits alone in *Xenopus* oocytes. We conclude that the I$_{Ks}$ channels have a higher single-channel conductance than channels from KvLQT1 alone, and that the sensitivity to external potassium ions is reflected in the size of single-channel currents in the case of the rhI$_{Ks}$ hybrid channel. The I$_{Ks}$ single-channel currents are roughly 0.6 pA at +50 mV. The relatively low conductance of these slowly activating channels might be important to reduce membrane potential fluctuations in cells where I$_{Ks}$ serves to shape long-duration action potentials.

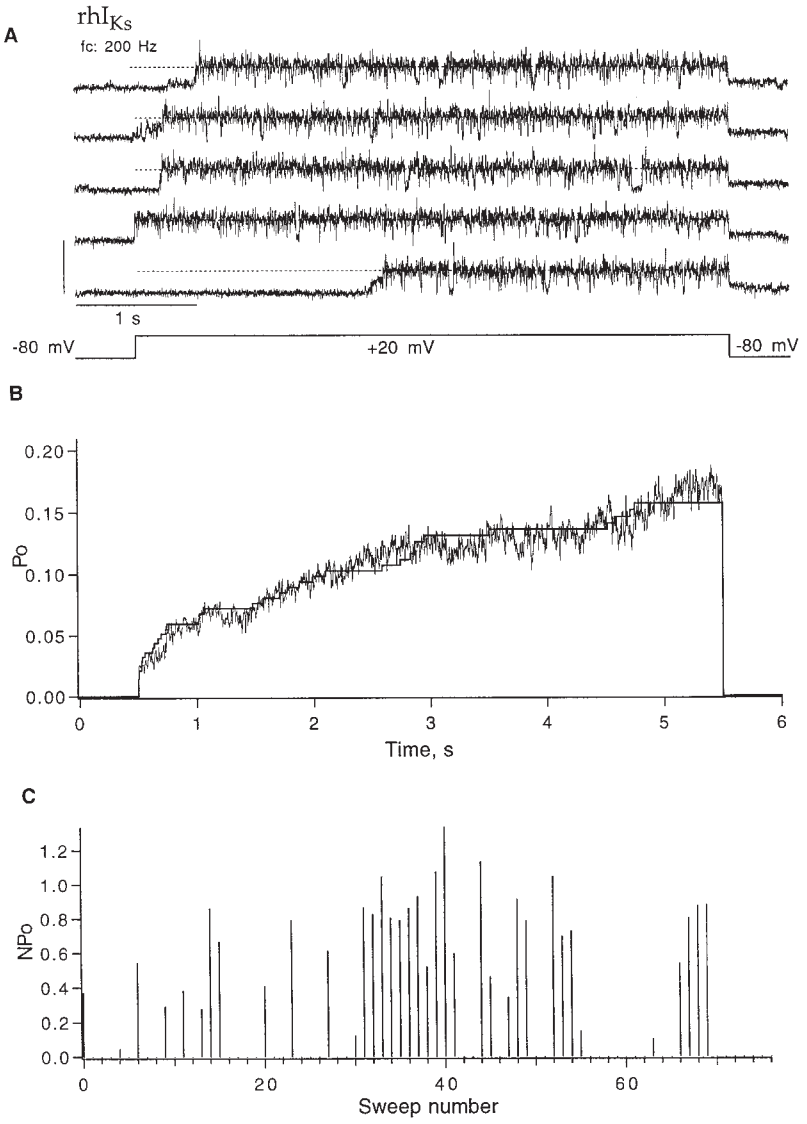

FIGURE 8. Behavior of rhI$_{Ks}$ channels at 20 mV; same three-channel patch as in Fig. 7. (*A*) Five successive sweeps showing activity from only one channel. (*B*) The ensemble mean time course obtained from 77 sweeps (*noisy trace*) shows an instantaneous onset followed by a slow activation phase. The maximum open probability was 0.17. Superimposed is the corrected one-channel first latency F_1 scaled by 0.8. (*C*) Diary plot of nP_o. Currents were elicited by depolarizations to +20 mV, 5-s duration, delivered at 8-s intervals from a holding potential of −80 mV. Of a total 77 sweeps, 37 showed some activity; 11 of those showed a second channel opening during depolarization, and one sweep showed three channels open simultaneously.

Size of Single-Channel Currents

The rapid flickering of currents in these channels makes difficult the determination of the single–open-channel current. When fluctuation analysis is used to estimate the single-channel current, the bandwidth of the recording must be sufficient to capture the fastest fluctuations, or else the variance will be underestimated, providing an underestimate of the single-channel current. The direct observation of single-channel currents suffers from a similar limitation: if a channel's current contains many brief interruptions, a single-channel recording at low bandwidth will show a reduced apparent single-channel current and increased apparent open probability. The very noisy appearance of the hI$_{Ks}$ recording at 500 Hz (Fig. 4 *A*) suggests that this bandwidth is not sufficient to resolve the true open-channel current. Fluctuation analysis allows a wider range of frequencies to be explored.

A two-state channel with opening and closing rate constants α and β yields current fluctuations having a Lorentzian power spectrum with a corner frequency $f_c = 1/2\pi(\alpha + \beta)$. Above f_c, the Lorentzian decays with frequency as f^{-2}; this relatively rapid decay means that the observed variance of the fluctuations converges rapidly to the correct value as the bandwidth is increased above f_c. On the other hand, no convergence results in the case of an f^{-1} frequency dependence, like that shown in Fig. 2 *E* for the hI$_{Ks}$ channels. Such a frequency dependence results in an observed variance that increases without limit as the bandwidth increases. Because bandwidth is related to the time scale of measurement, one could speak of an effective single-channel current value that depends on the time scale under which it is measured. Channels having stable open and closed states, such that the power spectrum of fluctuations from these channels decay rapidly at higher frequen-

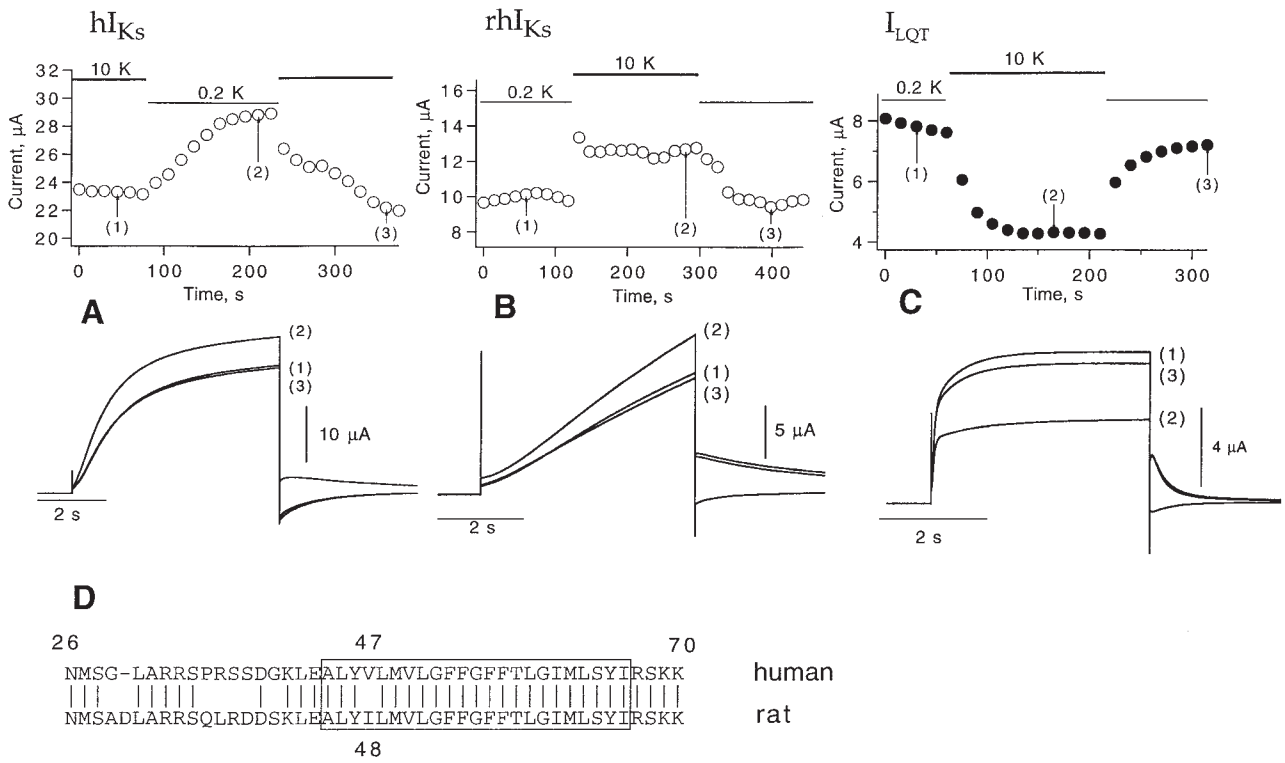

FIGURE 9. Effect of extracellular potassium on peak current of hI_{Ks}, rhI_{Ks}, and I_{LQT} in the two-electrode voltage clamp. (*A*) Magnitude of hI_{Ks} current at the end of 5-s depolarizations to +30 mV as the bath solution was switched between 0.2 and 10 mM K^+. The lower panel shows current traces corresponding to the times indicated at top. (*B*) rhI_{Ks} current; (*C*) I_{LQT} current; (*D*) the amino acid sequences of human and rat minK in the vicinity of the putative transmembrane region (*box*).

cies, show a distinct single-channel current value given sufficient recording bandwidth. For the hI_{Ks} channel, however, the 20-kHz limit of our power spectrum measurements was not sufficient to reach this regime. Thus we do not know the asymptotic value of the variance; we also do not know the exact open probability value that is necessary to correct the estimate of the single-channel current. The variance computed from fluctuations up to 20 kHz (Fig. 2), when corrected for an estimated absolute open probability of ~0.2, result in the estimated single-channel current of 0.6 pA at +50 mV, or a chord conductance of ~4.5 pS. These values are consistent with the current extremes observed in single-channel recordings (Fig. 4).

Another way to summarize the problem posed by the hI_{Ks} channel is that the very rapid current fluctuations make it difficult experimentally to distinguish, on the basis of time scales, between gating or channel-block phenomena on the one hand and the ion conduction process on the other. The apparent single-channel conductance values are influenced by the very rapid interruptions in the channel current.

The channels formed by hKvLQT1 subunits expressed alone or in combination with rat minK subunits showed less extreme behavior. Although the spectra of the current fluctuations are also very broad, they are not as featureless as those of hI_{Ks} currents and can be fitted by multiple Lorentzian components. Limiting single-channel current values at +50 mV of 0.09 and 0.84 pA are obtained from fluctuation analysis. These correspond to conductances of ~0.7 and 6.5 pS. The rhI_{Ks} channels resulting from coexpression were also

TABLE II

External K^+ Effect on Five Channel Types

Channels	hI_{Ks}	rI_{Ks}	LQT	hI_{Ks} (V471)	rI_{Ks} (I48V)
r, mean ± SD	0.72 ± 0.08	1.16 ± 0.07	0.67 ± 0.15	0.78 ± 0.12	0.91 ± 0.07
Oocytes tested	6	8	8	3	8

The parameter $r = I_{peak}(10\ K)/I_{peak}(0.2\ K)$ is the ratio of currents measured at the end of 5-s depolarizations to +30 mV with either 0.2- or 10-mM external potassium solutions bathing the oocyte. Oocytes were injected with the given constructs and currents were measured using the two-electrode voltage clamp.

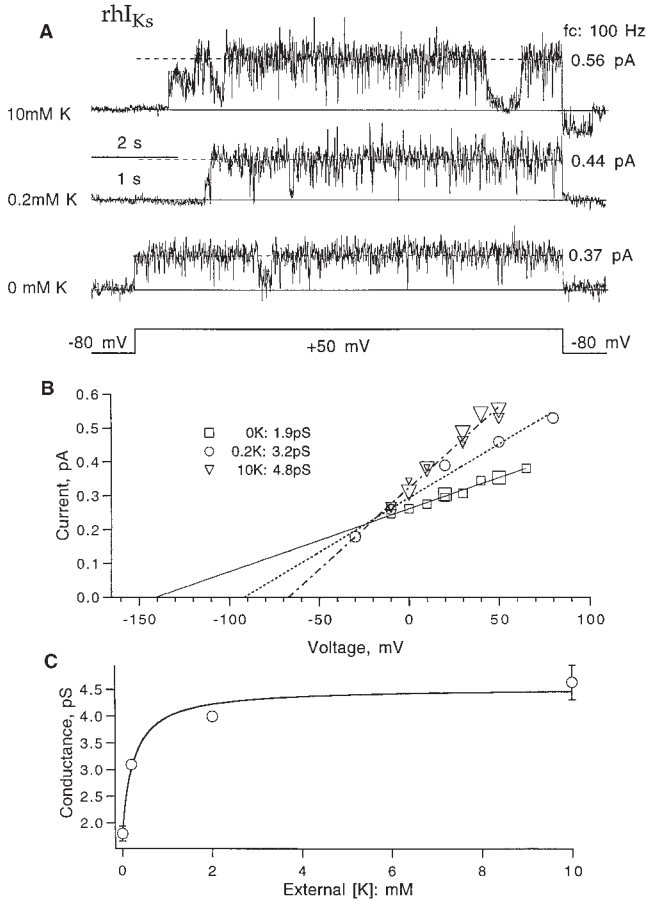

FIGURE 10. Single-channel conductance of rI$_{Ks}$ channels with different external K^+ solutions. (*A*) Representative current traces induced by +50-mV depolarizing pulses from −80-mV holding potential. Data were filtered at 100 Hz. (*B*) Single-channel current as a function of voltage obtained from double-Gaussian fits to amplitude histograms of traces. Fitted lines have slopes of 1.9, 3.2, and 4.8 pS for 0, 0.2, and 10 mM external K^+, respectively. (*C*) External potassium dependence of single channel conductance. Error bars represent SEM ($n = 2$ for 0 mM and $n = 4$ for 10 mM; the points at 0.2 and 2 mM K^+ are single observations). The superimposed fit is the function $\gamma = 1.8 + 2.8/(1 + 0.5\ \text{mM}/[\text{K}])$ pS.

observed directly from single-channel recording at 100 Hz bandwidth. There they appeared to have single-channel currents at +50 mV of ~0.5 pA, depending on extracellular K^+ concentration (Fig. 10).

In native tissues, the cardiac I_{Ks} current has been seen to have small fluctuations. Walsh et al. (1991) estimated unitary conductances of <1 pS in guinea pig myocytes. Taking into account their recording bandwidth of 200 Hz, we obtain a similar value. At 200 Hz, we would estimate a conductance of ~2 pS, as calculated from the estimated single-channel current at +50 mV of ~0.2 pA in both hI$_{Ks}$ and the hrI$_{Ks}$ channels (Figs. 2 *F* and 6 *C*).

It should be kept in mind that fluctuation analysis depends on several assumptions about the behavior of channels. We assume homogeneous populations of independently gating channels, and have also used the assumption that there is only one nonzero conductance level. It is likely that one or more of these assumptions is false. Evidence has been presented by Pusch et al. (1998) that KvLQT1 channels have two open states, and we see clear subconductance levels in single-channel recordings of the rhI$_{Ks}$ channels (Figs. 7 *B* and 8 *A*). If there are multiple conductance levels, the estimated single-channel current will lie between the largest and smallest single-channel current, and will depend on the probabilities of occupancy of the various conductance states. It should be kept in mind, however, that the high-conductance states tend to dominate the estimated conductance, because the contribution of a state's current i to the variance is proportional to i^2. Thus, our single-channel conductance estimates are likely to approximate the values for the largest conducting states.

A similar argument can be made concerning the possible heterogeneity of channel types. When minK and KvLQT1 cRNAs are coinjected, it is possible that hybrid channels are expressed having various stoichiometries, and the fluctuation analysis will give a weighted-average value. Again, it should be kept in mind that larger channel currents make larger contributions to the variance, and therefore predominate in the weighted average. Thus, if our coinjections produced a variety of channel types, the estimated conductance probably reflects the largest conductance value. Further, the good correspondence between the fluctuation analysis of rhI$_{Ks}$ currents and direct single-channel recordings argues that heterogeneity in channel conductances is not a serious problem.

How Coexpression of minK Affects KvLQT1 Current

Expression of KvLQT1 subunits produces small, rapidly activating potassium currents; coexpression of these with minK results in slowly activating I_{Ks} currents that are several-fold larger. These differences in the expressed currents have been seen in a variety of expression systems, including *Xenopus* oocytes, Sf9 cells, and in the mammalian cell lines CHO and COS (Barhanin et al., 1996; Sanguinetti et al., 1996; Romey et al., 1997). Is the increase in KvLQT1 current on coexpression with minK due to an increase in channel density or an increase in the single-channel current? Romey et al. (1997) addressed this question through single-channel recordings and noise analysis of expressed currents in COS cells. They concluded that the addition of minK subunits to KvLQT1 channels caused a reduction of single-channel conductance from 7.6 to 0.6 pS. To account for the increase in macroscopic current, they conclude that coexpression with minK causes the channel density to increase by a large factor, some 60-fold.

Our studies of these channels in *Xenopus* oocytes lead to the opposite conclusion, that a large part of the observed current increase on coexpression of minK arises

from an increase in single-channel conductance. From fluctuation analysis, we estimate a single-channel conductance of ~0.7 pS for KvLQT1 channels. We estimate the conductance of human I_{Ks} channels to be ~4.5 pS. The discrepancy between our results and those of Romey et al. (1997) might be explained by the difference between COS cell and oocyte expression systems. This, however, is unlikely because the behavior of the channels is similar in the various systems; further, Romey et al. (1997) report the same single-channel conductance value for I_{Ks} channels expressed in *Xenopus* oocytes as in COS cells.

Our results disagree with this previous work in two respects. First, we obtain a larger single-channel conductance for the human I_{Ks} channels than reported by Romey et al. (1997). This can be explained largely by the frequency dependence of fluctuations in this channel. Our value of 4.5 pS is based on fluctuation analysis at 20 kHz and on single-channel recordings at 500 Hz bandwidth; their value of 0.6 pS was based on fluctuation analysis at a bandwidth of 150 Hz under similar ionic conditions. Our conductance estimate of 6.5 pS for the closely related rhI_{Ks} channel (Figs. 6–10), for which openings are more readily resolved, supports the higher conductance estimate.

The other disagreement concerns the conductance of channels arising from the expression of KvLQT1 subunits alone. Romey et al. (1997) found well-resolved single-channel events in COS cells having a conductance of 7.6 pS. In our macropatch recordings, we find a remarkably noiseless current (Fig. 5). The power spectrum from the macropatch recording shows a broad frequency dependence, with a limiting conductance value of ~0.7 pS apparently being reached at 20 kHz bandwidth. There is always the danger that the currents in patch-clamp recordings are not properly identified, such that unitary events from one channel type are ascribed to another. Although we have not performed a pharmacological identification of our currents, we note that the kinetics of activation and the tail currents in our macropatch recordings agree very well with the currents observed from KvLQT1 channels in whole oocytes and in other expression systems (Fig. 1 *C*; Barhanin et al., 1996; Sanguinetti et al., 1996; Romey et al., 1997), supporting the view that it is these channels whose fluctuations we have measured.

Our results agree well with those of Sesti and Goldstein (1998), who studied channels expressed from KvLQT1 subunits alone and with human minK. They used symmetrical 100 mM potassium solutions and thereby obtained higher conductance values (4 and 16 pS) compared with ours (0.7 and 4.5 pS). Under the different ionic conditions, the single-channel outward currents are expected to be similar at large depolarizations. At +50 mV and 20 kHz bandwidth, our estimate for the single-channel current of hI_{Ks} channels is 0.6 ± 0.2 pA; here the error bounds reflect an estimate of statistical and systematic errors in the fluctuation analysis used. The corresponding estimate at 25 kHz bandwidth given by Sesti and Goldstein (1998) is 0.8 ± 0.2 pA.

Kinetics of I_{Ks} Channels

In addition to rapid flickering, the currents through single I_{Ks} channels show slow gating processes. At depolarizations to +20 and +50 mV (Figs. 7 and 8), the main determinant of the activation time course is seen to be the latency to first channel opening. In the rhI_{Ks} channels where single-channel events could be readily resolved, dwells in a subconductance state were often seen to precede full channel opening. The rhI_{Ks} channel activity also waxes and wanes on a time scale of ~30 s, as seen by groups of successive blank sweeps in patch recordings (Figs. 7 and 8).

The Conductance of minK "Channels"

The discovery that KvLQT1 subunits coassemble with the minK gene product to produce the I_{Ks} current (Barhanin et al., 1996; Sanguinetti et al., 1996) has clarified some of the puzzling aspects of the "I_{minK} current" that is seen in *Xenopus* oocytes when minK is expressed alone (Busch and Suessbrich, 1997). It is now clear that this current results from the combination of minK with an endogenous, *Xenopus* KvLQT1 homologue that is expressed at low levels (Sanguinetti et al., 1996). The difficulty that we and others have had in attempting to define the single-channel characteristics of I_{minK} are now understandable in view of the difficulties we have encountered in recording from single I_{Ks} channels. In a preliminary communication (Yang and Sigworth, 1995), we reported fluctuation analysis of a slowly activating current seen in patches from *Xenopus* oocytes, but many subsequent attempts were unsuccessful to establish this current as the same as the macroscopic, potassium-selective I_{minK}. It is possible that our patch currents, which from fluctuation analysis had a unitary current value below 1 fA, were contaminated with currents from an endogenous channel or ion transporter having slow kinetics, similar perhaps to the transporter studied by Schlief and Heinemann (1995).

We thank W.N. Joiner for the Bluescript-KSM vector and Y. Yan for cRNA preparation and oocyte injection. We also thank Dr. S.A.N. Goldstein for minK cDNA, and Drs. M. Sanguinetti and M. Keating for the human KvLQT1 cDNA.

Original version received 30 July 1998 and accepted version received 21 October 1998.

REFERENCES

Aldrich, R.W., D.P. Corey, and C.F. Stevens. 1983. A reinterpretation of mammalian sodium channel gating based on single channel recording. *Nature.* 306:436–441.

Attali, B., E. Guillemare, F. Lesage, E. Honore, G. Romey, M. Lazdunski, and J. Barhanin. 1993. The protein IsK is a dual activator of K^+ and Cl^- channels. *Nature.* 365:850–852.

Barhanin, J., F. Lesage, E. Guillemare, M. Fink, M. Lazdunski, and G. Romey. 1996. K(V)LQT1 and lsK (minK) proteins associate to form the I(Ks) cardiac potassium current. *Nature.* 384:78–80.

Ben-Efraim, I., Y. Shai, and B. Attali. 1996. Cytoplasmic and extracellular IsK peptides activate endogenous K^+ and Cl^- channels in *Xenopus* oocytes. Evidence for regulatory function. *J. Biol. Chem.* 271:8768–8771.

Blumenthal, E.M., and L.K. Kaczmarek. 1994. The minK potassium channel exists in functional and nonfunctional forms when expressed in the plasma membrane of *Xenopus* oocytes. *J. Neurosci.* 14:3097–3105.

Boyle, M.B., N.J. MacLusky, F. Naftolin, and L.K. Kaczmarek. 1987. Hormonal regulation of K^+-channel messenger RNA in rat myometrium during oestrus cycle and in pregnancy. *Nature.* 330: 373–375.

Busch, A.E., and H. Suessbrich. 1997. Role of the ISK protein in the IminK channel complex. *Trends Pharmacol. Sci.* 18:26–29.

Colquhoun, D., and F.J. Sigworth. 1995. Fitting and statistical analysis of single-channel records. *In* Single Channel Recording. 2nd ed. Plenum Publishing Corp., New York. 483–587.

Freeman, L.C., and R.S. Kass. 1993. Expression of a minimal K^+ channel protein in mammalian cells and immunolocalization in guinea pig heart. *Circ. Res.* 73:968–973.

Goldstein, S.A., and C. Miller. 1991. Site-specific mutations in a minimal voltage-dependent K^+ channel alter ion selectivity and open-channel block. *Neuron.* 7:403–408.

Hausdorff, S.F., S.A. Goldstein, E.E. Rushin, and C. Miller. 1991. Functional characterization of a minimal K^+ channel expressed from a synthetic gene. *Biochemistry.* 30:3341–3346.

Heinemann, S.H., and F. Conti. 1992. Nonstationary noise analysis and application to patch clamp recordings. *Methods Enzymol.* 207: 131–148.

Keating, M., C. Dunn, D. Atkinson, K. Timothy, G.M. Vincent, and M. Leppert. 1991. Consistent linkage of the long-QT syndrome to the Harvey ras-1 locus on chromosome 11. *Am. J. Hum. Genet.* 49:1335–1339.

Lesage, F., B. Attali, J. Lakey, E. Honore, G. Romey, E. Faurobert, M. Lazdunski, and J. Barhanin. 1993. Are *Xenopus* oocytes unique in displaying functional IsK channel heterologous expression? *Receptors Channels.* 1:143–152.

Marcus, D.C., and Z. Shen. 1994. Slowly activating voltage-dependent K^+ conductance is apical pathway for K^+ secretion in vestibular dark cells. *Am. J. Physiol.* 267:C857–C864.

Murai, T., A. Kakizuka, T. Takumi, H. Ohkubo, and S. Nakanishi. 1989. Molecular cloning and sequence analysis of human genomic DNA encoding a novel membrane protein which exhibits a slowly activating potassium channel activity. *Biochem. Biophys. Res. Commun.* 161:176–181.

Pusch, M., R. Magrassi, B. Wollnik, and F. Conti. 1998. Activation and inactivation of homomeric KvLQT1 potassium channels. *Biophys. J.* 75:785–792.

Romey, G., B. Attali, C. Chouabe, I. Abitbol, E. Guillemare, J. Barhanin, and M. Lazdunski. 1997. Molecular mechanism and functional significance of the minK control of the KvLQT1 channel activity. *J. Biol. Chem.* 272:16713–16716.

Sakagami, M., K. Fukazawa, T. Matsunaga, H. Fujita, N. Mori, T. Takumi, H. Ohkubo, and S. Nakanishi. 1991. Cellular localization of rat Isk protein in the stria vascularis by immunohistochemical observation. *Hear. Res.* 56:168–172.

Sanguinetti, M.C., M.E. Curran, A. Zou, J. Shen, P.S. Spector, D.L. Atkinson, and M.T. Keating. 1996. Coassembly of K(V)LQT1 and minK (IsK) proteins to form cardiac I(Ks) potassium channel. *Nature.* 384:80–83.

Sanguinetti, M.C., C. Jiang, M.E. Curran, and M.T. Keating. 1995. A mechanistic link between an inherited and an acquired cardiac arrhythmia: HERG encodes the IKr potassium channel. *Cell.* 81: 299–307.

Schlief, T., and S.H. Heinemann. 1995. H_2O_2-induced chloride currents are indicative of an endogenous Na^+–Ca^{2+} exchange mechanism in *Xenopus* oocytes. *J. Physiol. (Lond.).* 486:123–130.

Sesti, F., and S.A.N. Goldstein. 1998. Single channel characteristics of wild-type I_{Ks} channels and channels formed with two minK mutants that cause long QT syndrome. *J. Gen. Physiol.* 112:651–663.

Shalaby, F.Y., P.C. Levesque, W.P. Yang, W.A. Little, M.L. Conder, T. Jenkins-West, and M.A. Blanar. 1997. Dominant-negative KvLQT1 mutations underlie the LQT1 form of long QT syndrome. *Circulation.* 96:1733–1736.

Sigworth, F.J. 1980. The variance of sodium current fluctuations at the node of Ranvier. *J. Physiol. (Lond.).* 307:97–129.

Sigworth, F.J. 1981. Interpreting power spectra from nonstationary membrane current fluctuations. *Biophys. J.* 35:289–300.

Swanson, R., J. Marshall, J.S. Smith, J.B. Williams, M.B. Boyle, K. Folander, C.J. Luneau, J. Antanavage, C. Oliva, and S.A. Buhrow. 1990. Cloning and expression of cDNA and genomic clones encoding three delayed rectifier potassium channels in rat brain. *Neuron.* 4:929–939.

Tai, K.K., and S.A. Goldstein. 1998. The conduction pore of a cardiac potassium channel. *Nature.* 391:605–608.

Tzounopoulos, T., H.R. Guy, S. Durell, J.P. Adelman, and J. Maylie. 1995. minK channels form by assembly of at least 14 subunits. *Proc. Natl. Acad. Sci. USA.* 92:9593–9597.

van den Berg, M.H., A.A. Wilde, E.O. Robles de Medina, H. Meyer, J.L. Geelen, R.J. Jongbloed, H.J. Wellens, and J.P. Geraedts. 1997. The long QT syndrome: a novel missense mutation in the S6 region of the KVLQT1 gene. *Hum. Genet.* 100:356–361.

Varnum, M.D., A.E. Busch, C.T. Bond, J. Maylie, and J.P. Adelman. 1993. The minK channel underlies the cardiac potassium current I_{Ks} and mediates species-specific responses to protein kinase C. *Proc. Natl. Acad. Sci. USA.* 90:11528–11532.

Walsh, K.B., J.P. Arena, W.M. Kwok, L. Freeman, and R.S. Kass. 1991. Delayed-rectifier potassium channel activity in isolated membrane patches of guinea pig ventricular myocytes. *Am. J. Physiol.* 260:H1390–H1393.

Wang, K.W., and S.A. Goldstein. 1995. Subunit composition of minK potassium channels. *Neuron.* 14:1303–1309.

Wang, K.W., K.K. Tai, and S.A. Goldstein. 1996*a*. MinK residues line a potassium channel pore. *Neuron.* 16:571–577.

Wang, Q., M.E. Curran, I. Splawski, T.C. Burn, J.M. Millholland, T.J. VanRaay, J. Shen, K.W. Timothy, G.M. Vincent, T. de Jager, et al. 1996*b*. Positional cloning of a novel potassium channel gene: KVLQT1 mutations cause cardiac arrhythmias. *Nat. Genet.* 12:17–23.

Yang, W.P., P.C. Levesque, W.A. Little, M.L. Conder, F.Y. Shalaby, and M.A. Blanar. 1997. KvLQT1, a voltage-gated potassium channel responsible for human cardiac arrhythmias. *Proc. Natl. Acad. Sci. USA.* 94:4017–4021.

Yang, Y., and F.J. Sigworth. 1995. The conductance of minK 'channels' is very small. *Biophys. J.* 68:*A*22.